Fourier Transform Infrared Spectroscopy (FTIR) and X-Ray Diffraction Analyses of Mineral and Organic Matrix During Heating of Mother of Pearl (Nacre) from the Shell of the Mollusc *Pinctada maxima*

J. Balmain,[1] B. Hannoyer,[1] and E. Lopez[2]

[1] Laboratoire d'Analyse Spectroscopique et de Traitement de Surface des Matériaux, LASTSM—IUT, Université de Rouen, 76821—Mont Saint-Aignan Cedex, France

[2] URA90 CNRS, Muséum National d'Histoire Naturelle, 7, rue Cuvier, 75231 Paris, Cedex 05, France

Received 8 June 1998; revised 30 November 1998; accepted 25 January 1999

Abstract: Fourier transform infrared spectroscopy (FT-IR) and X-ray diffraction patterns were used to analyze the mineral structure and organic matrix composition and thermal behavior of the internal nacreous layer (mother of pearl or nacre) of the shell of the giant oyster *Pinctada maxima*. Nacre is a natural biomaterial with osteogenic properties. The mineral of nacre is calcium carbonate crystallized as aragonite and it is highly crystallized. The FT-IR spectra showed amide, amine, and carboxylic acid groups in the organic matrix of the whole (organic and mineral) nacreous layer, with the HCO_3^- groups possibly at the organic-mineral interface. The insoluble organic matrix remaining after decalcification contained amide, amine, and carboxylic groups. The heated aragonite mineral structure of nacre underwent two transformations (X-ray diffraction), aragonite to calcite at 300–400°C, and calcite to calcium oxide (CaO) at 500–600°C. The organic matrix of nacre was destroyed around 550–600°C, the same temperature as the calcite to CaO transformation, revealing the great thermal stability of the organic matrix and the organic-mineral bonding. This could be an useful feature for the *in vivo* use of this natural biomaterial as an implant. © 1999 John Wiley & Sons, Inc. J Biomed Mater Res (Appl Biomater) 48: 749–754, 1999

Keywords: mother of pearl (nacre); FT-IR spectroscopy; X-ray diffraction; thermal behavior

INTRODUCTION

The structure and mineralogy of the shells of bivalve [1,2] and gasteropod [3] mollusks have been extensively studied. The shell is composed of an organic matrix and a mineral phase with an external layer, generally of calcified units (calcite), and an internal nacreous or pearly layer consisting of sheets of calcium carbonate (aragonite) separated by organic matrix .[4]

The inner part of the shell, nacre (mother of pearl), of the giant oyster *Pinctada maxima* has a lamellar 3-dimensional structure, giving it a high density. It has been used as a natural material for bone replacement and regeneration in human maxillary alveolar bone defects,[5] and as a bone substitute in sheep.[6] Nacre is biocompatible, has osteogenic and osteoinductive properties,[7] and can initiate bone formation by human osteoblasts *in vitro*.[8,9] It has also been implanted in the midshafts of rat bone.[10] This is an entirely new phenomenon. Bobbio[11] reported that the Maya Indians of Honduras used Mother of pearl (nacre) as a dental implant 2000 years ago. Recent studies show that adding heated oyster shell and seaweed to the diet of the elderly patients (65–96 years) appears to increase the bone mineral density (BMD) of the lumbar spine.[12]

Several materials have been used in orthopedic and maxillofacial surgery over the past decade or so.[13,14] Most of them have been metals, but polymers, ceramics, and carbon-based materials have also been used.[14] There have been few materials of biological origin. Those that have been used include coral, which is a porous natural ceramic,[15–19] and nacre or mother of pearl. The main crystal structure in both of them is aragonite.

There is considerable need to understand how mother of pearl may be actively involved in hard-tissue regeneration, for both bone and other applications. A fundamental step is a sound knowledge of its physico-chemical properties. The present study was, therefore, undertaken to evaluate the physico-chemical composition and thermal behavior of the

Correspondence to: J. Balmain, Laboratoire d'Etude des Matériaux en Milieux Agressifs, LEMMA, Université de La Rochelle, Pôle Sciences et Technologie, Avenue Marillac, 17042 La Rochelle Cedex, France (e-mail: jbalmain@univ-lr.fr) and E. Lopez (e-mail: lopez@mnhn.fr)

 CCC 0021-9304/99/050749-06

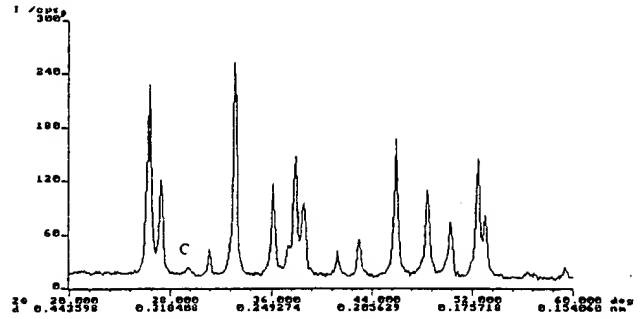

Figure 1. X-ray diffraction pattern of powdered nacre (mother of pearl) from *Pinctada maxima* corresponding to typical data for aragonite with a trace of (c) calcite.

mineral and organic phases of the internal nacreous layer of *Pinctada maxima* using X-ray diffraction and Fourier transform infrared spectroscopy.

MATERIALS AND METHODS

Materials

Specimens of the giant tropical oyster, *Pinctada maxima*, were collected in French Polynesia. The shells were washed, air-dried, and stored. They have three layers: the periostracum, the mosaic of prismatic calcite units, and the inner nacreous layer of mother of pearl (nacre). The inner nacreous layer was removed, cut into pieces, and ground into particles (50—100 μm), in a agate bead grinder by The Center for Technology Transfers in Ceramics (Limoges, France). Grinding was done at ambient temperature to avoid thermal breakdown and under dry conditions to avoid dissolving out components of the organic matrix. The resulting powder was stored at room temperature.

Material Preparation

Some samples of the nacreous layer powder were used undecalcified; others were decalcified by placing them in 0.1M EDTA (pH 7.4) or in 1M acetic acid /ethanol (v/v) pH 4, at room temperature with gentle stirring. The salts were removed from EDTA-treated samples by washing with buffered water (pH 7.4), and from the acetic/ethanol-treated samples with ethanol. The insoluble organic matrix was air-dried.

Analytical Methods

X-ray diffraction patterns were recorded on a Seifert XRD7 diffractometer using CuK_α radiation (λ = 0.154 nm).

The Fourier transform infrared spectra (FT-IR) of all specimens, undecalcified and decalcified, were recorded at 4 cm^{-1} resolution with 64 scans on a Nicolet 710 spectrophotometer equipped with a diffuse reflectance accessory. The powder was mixed with KBr (1:100 ratio) in an agate mortar. Spectra were automatically corrected with the KBr background to minimize the CO_2 and H_2O absorptions and recorded from 4 000 cm^{-1} to 280 cm^{-1}.

Thermal decomposition of undecalcified powered nacre.

Nacre powder (100 mg) in a crucible was placed in an oven set at the experimental temperature and heated in air from 250–900°C: 13 h at 250–550°C and 5 h at 600–900°C. The residues were weighted (Mettler Toledo AG 245 balance, 10^{-5} g sensitivity).

RESULTS AND DISCUSSION

X-ray Diffraction of Unheated Nacre Powder

The X-ray diffraction pattern of the *Pinctada maxima* nacre (Fig. 1) had all the characteristic diffraction lines of aragonite according to specifications JCPDS n°41–9475. The X-ray diffraction pattern had the very sharp lines characteristic of a well-crystallized mineral. Despite the presence of a very light line at d = 0.3035 nm, 2θ = 29.4 deg. (c in Fig. 1) due to a small quantity of calcite (JCPDS n°47–1743), there was a single mineral phase that crystallized into an aragonic structure. The trace of calcite could be due to the transformation of aragonite to calcite due to local heating during grinding, a small amount of calcite in the nacre itself, or contamination with calcite from the external layer during sampling.

FT-IR Analysis of Unheated Nacre Powder

Figure 2 shows the whole nacre layer composed of an organic matrix and mineral phase. Both of them gave numerous bands from 4000 cm^{-1} to 280 cm^{-1}. The carbonate ions in the mineral were demonstrated by the internal vibration modes of the CO_3^{2-} ions, 713, 700 (ν_4) – 864, 844 (ν_2) – 1090 (ν_1) and 1490 (ν_3) cm^{-1}. The strong IR band detected at 1792 cm^{-1} could also be attributed to the C=O groups of the carbonate ions. The splitting of ν_4 is characteristic of aragonite structure. The broad, strong band at 288 cm^{-1} is consistent with the translational mode frequencies of the carbonates of the aragonite structure, including the longitudinal and transverse modes. The strongest absorption band of the mineral in the ν_3 region was overlapped by the absorption of the

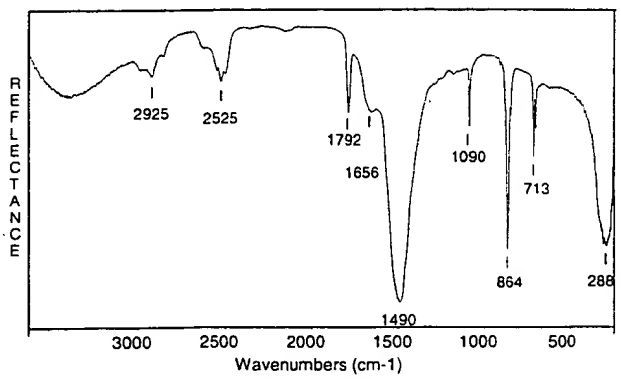

Figure 2. FT-IR spectrum (reflectance) of powdered nacre (mineral and organic matrix) from *Pinctada maxima*.

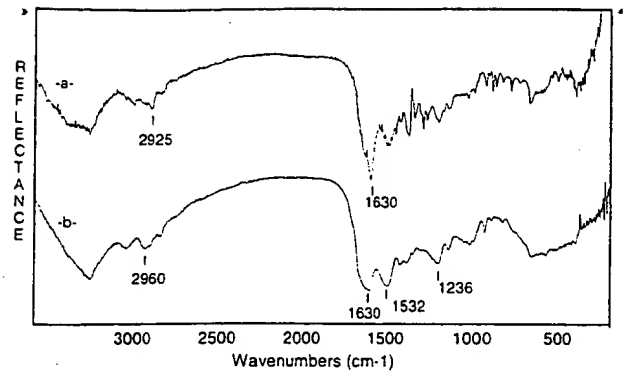

Figure 3. FT-IR spectra of the insoluble organic matrix of the powdered nacre from *Pinctada maxima*, decalcified with (a) EDTA or (b) acetic acid.

organic matrix. This was corroborated by the FT-IR spectra of material decalcified by EDTA [Fig. 3(a)] or acetic acid [Fig. 3(b)], which had very intense absorption bands in the range 1660 – 1100 cm^{-1}.

While the aim of this study was not to determine the components of the organic matrix of nacre, the IR spectrum of EDTA decalcified material [Fig. 3(a)], thus of the insoluble organic matrix, revealed the same bands in the ranges 3200–3500 cm^{-1} and 2800– 3000 cm^{-1} as the IR spectrum of undecalcified nacre powder (Fig. 2). The OH and/or NH stretching modes of the organic matrix components were found in the region 3000–3500 cm^{-1}, while the C—H stretching modes were assigned to the 2800–3000 cm^{-1} region.

The strong IR bands at 1630 and 1660 cm^{-1}(shoulder) on Fig. 3, which correspond to the band at 1656 cm^{-1} of the undecalcified nacreous layer powder (Fig. 2), were attributed to the amide I (C—O bond) and /or amide II (C—N bond) groups of the organic matrix proteins. This is in agreement with the findings of Dauphin and Marin[20] for the organic matrix of several cephalopod skeletons. The bands at 1630–1660 cm^{-1} could not be due to residual EDTA, since they also occurred in material decalcified with acetic acid [Fig. 3(b)]. The bands at 1532 cm^{-1} and 1236 cm^{-1} were more intense in acetic acid decalcified material than in material decalcified with EDTA (Fig. 3). They can be attributed to the amide II and III groups of the proteins. These results are also in agreement with the results of Dauphin and Marin[20] for crustacean chitin.

Another absorption area of the undecalcified nacre powder spectrum (Fig. 2) was attributed to the organic matrix. These are the bands in the range 2520–2650 cm^{-1}, which may be due to the OH groups of carboxylic acids. These groups may be removed with the soluble matrix during decalcification. The bands did not appear in the insoluble organic matrix spectra after decalcification [Figs. 3(a) and (b)]. The absence of these bands from the organic matrix after decalcification (EDTA and acetic acid/ethanol) is not surprising, because amino acid analyses of the water-soluble matrix of Pinctada margaritifera var-cumigi nacre show that it has a high concentration of acidic carboxylic amino acids (aspartic and glutamic acids).[21] Our data on the organic matrix are for the insoluble organic matrix after acetic acid/ethanol and EDTA decalcification, and not the water-soluble matrix. The IR band characteristic of carboxylate groups at 1420 cm^{-1} was also found for the cephalopod soluble matrix.[20]

HCO_3^- groups could also contribute to the observed absorption in the 2520–2650 cm^{-1} range by absorption due to OH groups expected around 2600 cm^{-1}. These groups are probably in the soluble components of the organic matrix, since they are not on the FT-IR spectra of decalcified nacre (Fig. 3). Sabbides and Koutsoukos[22] studying the formation of calcium carbonate in artificial seawater used synthetic seed crystals and detected the characteristic bands of aragonite at 1785 and 1080 cm^{-1}. But their spectra also showed bands at 2500–2650 cm^{-1} and bands near 2900 cm^{-1}, exactly as we have found; but these authors made no reference to such bands. We suggest that the bands at 2520–2650 cm^{-1} in the spectrum of the whole (organic and mineral) nacreous layer of *Pinctada maxima* are due to the HCO_3^- in the mineral and/or at the organic-mineral interface, as the bands were not detectable after decalcification. We detected no bands at 2500–2650 cm^{-1} on the IR spectra of the nacre water-soluble matrix (Balmain et al., unpublished results). Belcher et al.[23] used hypochlorite to study the mollusk-shell proteins of the abalone, and found that oxidation of the extra-crystalline proteins, before demineralization of the shell, protected one of the aragonite proteins from oxidative destruction by hypochlorite. They conclude that this protein is intracrystalline. Miyamoto et al.[24] analyzed the soluble organic matrix of the nacre of the pearl oyster, P. fucata, and found that the proteins contained two functional domains: one an acidic Gly-Asp, Asn, or Glu domain, and the other a carbonic anhydrase domain. This enzyme catalyzes the formation of HCO_3^-. These authors suggest that the carbonic anhydrase in nacre catalyses the formation of HCO_3^- and, thus, participates in calcium carbonate crystal formation. They suggested that HCO_3^- is an intermediate in the formation of calcium carbonate crystals by "nacrein."

We, therefore, propose that the bands at 2520–2650 cm^{-1}, found only in the whole (organic and mineral) nacreous layer of *Pinctada maxima*, are due to HCO_3^- groups in the crystal lattice or at the mineral/organic interface.

Thermal Behavior of Powdered Nacre

Weight Changes. The loss of weight of nacreous powder heated from 250–900°C is shown in Fig. 4. The loss was quite constant (about 4% wt) up to 500°C, while the loss from 700–900°C was about 50%. Therefore, the greatest weight loss (about 46% wt) occurred at 500–600°C, indicating that a transformation occurred at this temperature. The nature of this transformation is shown by X-ray diffraction patterns (Fig. 5) and FT-IR spectroscopy (Fig. 6) data for heated nacre powder and discussed later.

X-ray Diffraction. The X-ray diffraction patterns of the nacre powder heated from 250–900°C are shown in Fig. 5.

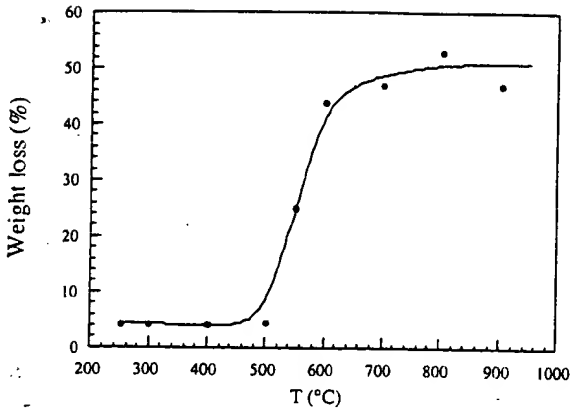

Figure 4. Loss of weight from powdered nacre from *Pinctada maxima*, heated from 250–900°C.

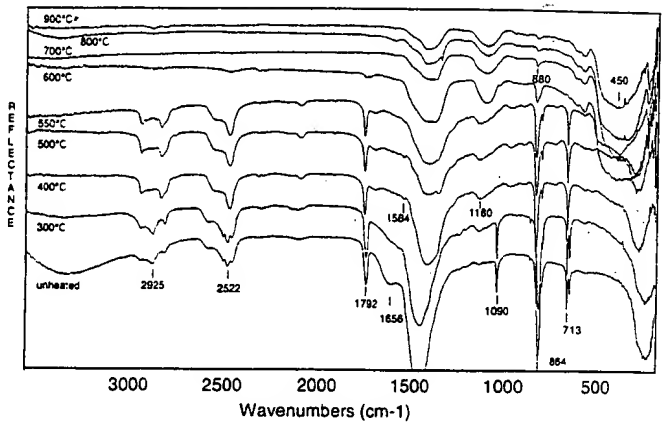

Figure 6. FT-IR spectra of unheated and heated (300–900°C) samples of nacre of *Pinctada maxima*.

Only the mineral phase is detected by this technique. The nacre powder at 250°C and 300°C had the same aragonite structure as the unheated powder (Fig. 1). The diffraction line of calcite was slightly more prominent at 250°C and 300°C, but the general structure remained mainly aragonitic. The mineral changed from aragonite to calcite at 300–400°C. The lines of the aragonite disappeared and the mineral of nacre powder became purely calcite [Fig. 5(c)].

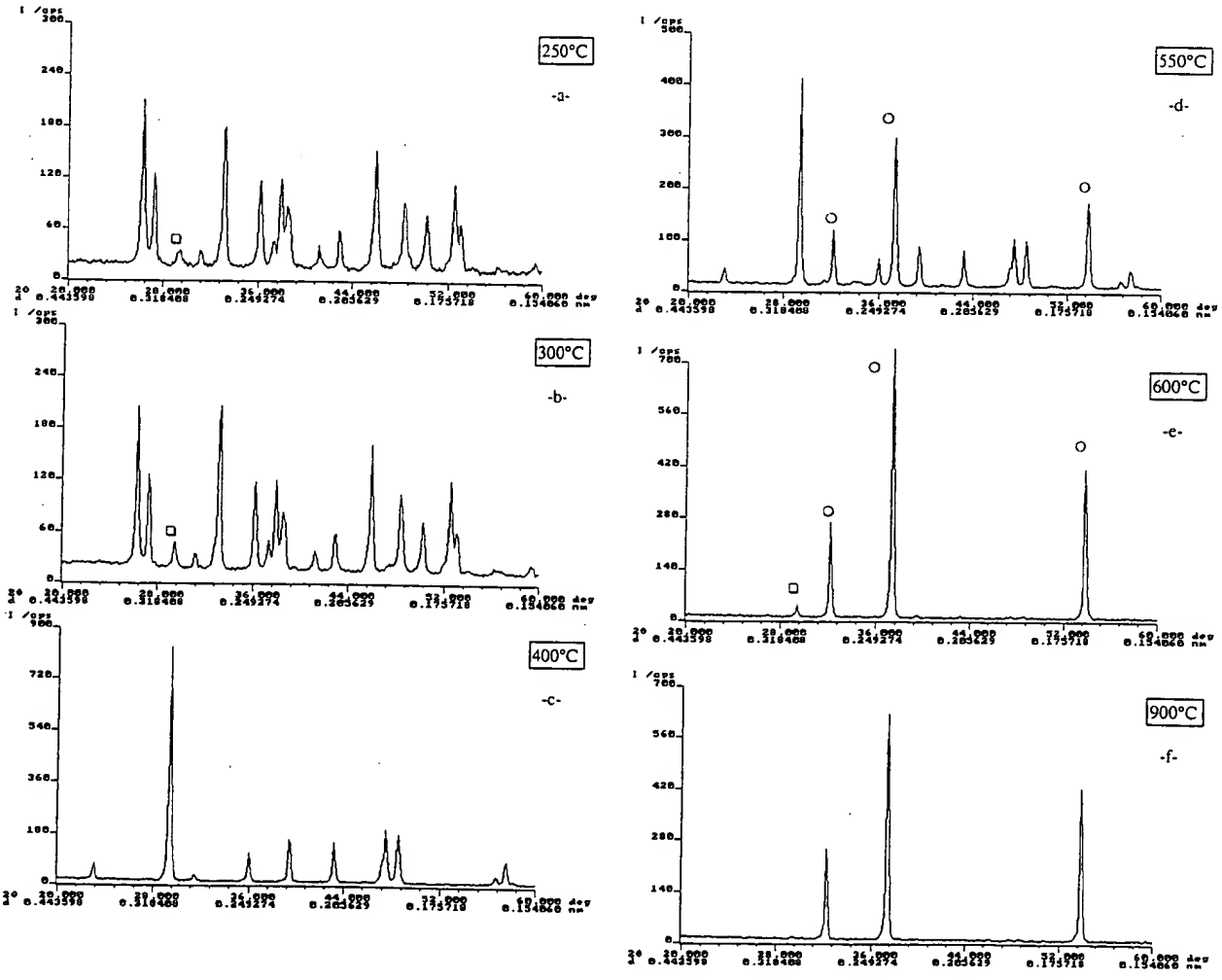

Figure 5. X-ray diffraction patterns of powdered nacre from *Pinctada maxima*, heated from 250–900°C: 250 and 300°C: aragonite and traces of calcite (□) ; 400°C: calcite; 550°C: calcite and CaO (○); 600°C: CaO (○) and calcite (□); 900°C : CaO.

Then, in agreement with the weight loss (Fig. 4), there was a second transformation at 500–600°C [Fig. 5(d)]. The X-ray diffraction pattern at 550°C clearly showed two constituents, calcite and CaO (JCPDS n° 40–777). Although the transformation was not complete after heating for 5 h at 600°C [Fig. 5(e)], the powder was mainly calcium oxide, CaO. The transformation of calcite to CaO was accompanied by the release of CO_2, which accounts for the weight loss at 500–600°C (Fig. 4). In fact, the 46% weight loss in this range of temperature is in good agreement with the theoretical loss of 44 wt% when CO_2 is eliminated. Finally, only tiny traces of calcite were detected at 900°C, and the material was then entirely transformed into CaO with the loss of CO_2.

Fourier Transform Infrared Spectra. The FT-IR spectra for undecalcified nacre powder heated from 300–900°C and the spectrum of the unheated powder are shown in Fig. 6. The change in the initial characteristic carbonate bands ν_1 (1090 cm^{-1}), ν_2 (864,844 cm^{-1}), and ν_4 (713,700 cm^{-1}) with increasing temperature confirmed the X-ray diffraction findings for the aragonite-calcite transformation at 300–400°C (Fig. 5). The transformation from aragonite to calcite[25] was shown by the ν_1 vibration detected from room temperature to 300°C and lost at 400°C, by the shift from 864 to 880 cm^{-1} of the band in the ν_2 region and by the degenerency of ν_4, which is completely broken down at room temperature and at 300°C, indicating aragonite, while the single band at 713 cm^{-1} at 400°C confirmed the calcite structure. The second transformation, from calcite to CaO, detected on the X-ray diffraction pattern (Fig. 5), was also clearly shown by changes in the IR spectrum in the 600–900°C range. The decreased carbonate content was indicated by the lower intensity of the characteristic band at 880 cm^{-1}(ν_2). The spectrum at 900°C was that of CaO with the main broad absorption at 450 cm^{-1}.[26]

As mentioned earlier, the best indicator of the organic matrix in the nacre powder were the bands at 2800–3000 cm^{-1}, characteristic of the C—H bonds (Fig. 2). These bands were modified as the temperature increased, but were still present at 550°C. They were lost at 600°C, indicating that all the organic matrix had then been destroyed. This destruction of the nacreous organic matrix also contributed to the weight loss between 500–600°C (Fig. 5) and to the difference between the theoretical and experimental weights. However, it was not possible to accurately estimate the percentage weight of the organic matrix of nacre by this method, because the organic matrix was lost at the same time that CO_2 was released during the calcite–CaO transformation. Other information on the thermal behavior of the organic matrix was obtained from the gradual decrease in the intensity of the band at 1656 cm^{-1} from room temperature to 600°C, representing the degradation of amide groups. The bands at 1180 cm^{-1} and 1584 cm^{-1}, due to amine groups, became more visible from 300–550°C.

Nacre and Bone

Bone mineral is a poorly crystalline carbonate and acidic-phosphate-apatite (hexagonal crystal)[27-35] that is quite different from the well-crystallized calcium carbonate of aragonite (rhombohedral crystal) in the nacreous layer of the oyster shell. However, the mineral phases of both bone and nacre contain carbonate ions, and nacre can be dissolved in the body and resorbed, making it an effective bone substitute. Carbonate is important in bone for dissolution of the apatite mineral.[36] The carbonates in the apatite lattice decrease the stability of the apatite structure, increasing its solubility in acid.[37] The present data show that the thermal behavior of carbonate ions of nacre is quite different from that of bone. Carbonate ions are removed from nacre in a single step, at 500–600°C, while they are released in two stages from bone, first at 200–300°C and then at 600–700°C,[29] probably because there are carbonate ions at PO_3^- sites (type B carbonate), and others substituting for OH (type A carbonate), in the apatite structure of bone.[31]

The thermal decompositions of the organic matrices of bone and nacre are also quite different. The bone matrix begins to be destroyed from 200°C and is entirely decomposed at 500°C, [30] while the nacre organic matrix is not destroyed until 550°C, at the same temperature as carbonate ions are eliminated from the mineral, revealing that both the organic matrix and the mineral of nacre are much more thermally stable. This behavior shows that it is possible to sterilized nacre for use as an implant at temperatures up to 300°C, at which temperature the two components of nacre (organic matrix and mineral) are still intact. No significant transformations of the organic matrix or the aragonite structure occur below 300°C, when aragonite is transformed to calcite, a more thermodynamically stable phase.

CONCLUSIONS

We find that the mineral of the nacreous layer of *Pinctada maxima* shell is calcium carbonate crystallized as aragonite. It is a well-crystallized single mineral phase unlike the mineral of bone, which is a poorly crystallized acidic phosphate-carbonated-apatite. The mineral in nacre undergoes two transformations when heated. The first is from aragonite to calcite at 300–400°C, with no change in weight and no loss of either organic or mineral material. The second transformation, from calcite to CaO at 500–600°C, is accompanied by the loss of CO_2 from the mineral phase.

The FT-IR spectra of whole nacre powder and decalcified nacre powder show that there are several functional groups (amide, amine, carboxylic acids) in the whole material (organic matrix and mineral) and in the insoluble organic matrix (amide, amine). HCO_3^- groups can be detected in the whole (organic and mineral) of nacre, but not after decalcification, suggesting an interaction with crystal. The results also indicate that the organic matrix of the whole undecalcified nacre remains present up to a high temperature, although it may be

slightly altered during the aragonite–calcite mineral transformation at 300–400°C. The organic matrix is destroyed only at around 550–600°C, when the mineral is transformed to calcium oxide, CaO, showing a strong interaction between the organic and the mineral phases. Thus, the nacreous organic matrix is strongly linked to the mineral and has a much greater thermal stability than the organic matrix of bone, which may be important for the future use of nacre as a biomaterial for surgical bone repair.

The authors thank Prof. J. Lopitaux for his contribution to the X-ray diffraction (LASTSM) , Dr. O. Parkes for checking the English of the manuscript, and F. Lallier (URA90 CNRS) for secretarial assistance.

REFERENCES

1. Taylor JD, Kennedy WJ, Hall A. The shell structure and mineralogy of the bivalvia. Introduction. Nuculacea — Trigonacea. Bull British Museum Zoolog Suppl 1969;3:4–90.
2. Mutvei H. The nacreous layer in mytilus, nucula and unio (bivalvia). Crystalline composition and nucleation of nacreous tablets. Calcif Tissue Res 1977;24:11–18.
3. Mutvei H. Ultrastructural characteristics of the nacre in some gastropods. Zoologica scripta 1978;7:287–296.
4. Manne S, Zaremba CM, Giles R, Huggins L, Walters DA, Belcher A, Morse DE, Stucky GD, Didymus JM, Mann S, Hansma PK. Atomic force microscopy of the nacreous layer in mollusk shells. Proc R Soc Lond 1994;256B:17–23.
5. Atlan G, Balmain N, Berland S, Vidal B, Lopez E. Reconstruction of human maxillary defects with nacre powder: histological evidence for bone regeneration. CR Acad Sci Paris 1997;320:13–18.
6. Delattre O, Catonne Y, Berland S, Borzeix S, Lopez E. Use of mother of pearl as a bone substitute. Experimental study in sheep. Eur J Orthop Surg Traumatol 1997;7:1–5.
7. Lopez E, Berland S, LeFaou A. Nacre, osteogenic and osteoinductive properties. Bull de l'Inst Océano Monaco 1995;3:49–57.
8. Lopez E, Vidal B, Berland S, Camprasse S, Camprasse G, Silve C. Demonstration of the capacity of nacre to induce bone formation by human osteoblasts maintained in vitro. Tissue Cell 1992;24:667–679.
9. Silve C, Lopez E, Vidal B, Smith DC, Camprasse S, Camprasse G, Couly G. Nacre initiates biomineralization by human osteoblasts maintained in vitro. Calcif Tissue Int 1992;51:363–369.
10. Liao H, Brandsten C, Lundmark T, Li J. Responses of bone to titania-hydroxyapatite composite and nacreous implants: a preliminary comparison by in situ hybridization. J Mat Sci Mater Med 1997;8:823–827.
11. Bobbio A. The first endosseous alloplastic implant in the history of man. Bull Hist Dent 1972;20:1–6.
12. Fujita T, Ohue T, Fujii Y, Miyauchi A, Takagi Y. Heated oyster shell-seaweed calcium (AAA Ca) on osteoporosis. Calcif Tissue Int 1996;58:226–230.
13. Nizard R, Bizot P, Kerboull L, Sedel L. Biomatériaux orthopédiques. Encycl Med Chir, Techniques chirurgicales — Orthopédie — Traumatologie, 44–003. Paris: Elsevier; 1996. p 20.
14. Sedel L, Rey C. Bioceramics. Vol. 10. Paris: Pergamon (Elsevier Science), 1997.
15. Guillemin G, Fournie J, Patat JL, Chetail M. Contribution á l'étude du devenir d'un fragment de squelette de corail madrépore implanté dans la diaphyse des os longs chez le chien. CR Acad Sci Paris 1981;293:371–376.
16. Guillemin G, Meunier A, Dallant P, Christel P, Pouliquen JC, Sedel L. Comparison of coral resorption and bone apposition with two naturals of different porosites. J Biomed Mater Res 1989;23:765–779.
17. Patat JL, Pouliquen JC, Guillemin G. Le corail naturel utilisé comme substitut de greffon osseux. In: Mainard D, Delagoutte JP, Merle M, editors. Application clinique en chirurgie orthopédique et traumatologique. Actualités en biomatériaux. Paris: Romillat; 1990. p 161–175.
18. Irigaray JL, Braye F, Oudadesse H, Jallot E, Weber G, Amiribadi A, Tixier H. Diffusion of mineral elements evaluated by PIXE at the bone-coral interface. J Biomater Sci Polymer Ed 1996;7:741–749.
19. Fricain JC, Baquey C, Basse–Cathalinat B, Dupuy B. Comparison of resorption and bone conduction of two $CaCO_3$ bone substitutes. In: Sedel L, Rey C, editors. Bioceramics. Vol. 10. London: Elsevier Science; 1997. p 383–387.
20. Dauphin Y, Marin F. The compositional analysis of recent cephalopod shell carbohydrates by Fourier transform infrared spectrometry amperometric detection. Experentia 1995;51:278–283.
21. Cuif JP, Dauphin Y. Occurrence of mineralization disturbances in nacreous layers of cultivated pearls produced by Pinctada margaritifera var. cumingi from French Polynesia. Comparison with reported shell alterations. Aquat Liv Resour 1996;9:187–193.
22. Sabbides TG, Koutsoukos PG. The crystallization of calcium carbonate in artificial seawater; role of the substrate. J Cryst Growth 1993;133:13–22.
23. Belcher AM, Wu XH, Christensen RJ, Hansma PK, Stucky GD, Morse DE. Control of crystal phase switching and orientation by soluble mollusk-shell proteins. Nature 1996;381:56–58.
24. Miyamoto H, Miyashita T, Okushima M, Nakano S, Morita, T. A carbonic anhydrase from the nacreous layer in oyster pearls. Proc Natl Acad Sci USA 1996;93:9637–9660.
25. Ross SD. Inorganic infrared and raman spectra. London: McGraw–Hill; 1972.
26. Nyquist RA, Kagel RO. Handbook of infrared and raman spectra of inorganic compounds and organic salts. San Diego: Academic; 1971.
27. Termine JD, Lundy DR. Hydroxide and carbonate in rat bone mineral and its synthetic analogues. Calcif Tissue Res 1973;13: 73–82.
28. Posner AS, Blumental NC, Boskey AL, Betts F. Synthetic analogue of bone mineral formation. J Dent Res 1975;54:B88–B93.
29. Legros R, Balmain N, Bonel G. Structure and composition of the mineral phase of periosteal bone. J Chem Res (S) 1986;9: 8–9.
30. Legros R, Balmain N, Bonel G. Age-related changes in mineral of rat and bovine cortical bone. Calcif Tissue Res 1987;41:137–144.
31. Rey C, Collins B, Goehl T, Dickson IR, Glimcher MJ. The carbonate environment in bone mineral: a resolution enhanced Fourier transform infrared spectroscopy study. Calcif Tissue Int 1989;45:157–164.
32. Rey C, Shimizu M, Collins B, Glimcher MJ. Resolution-enhanced Fourier transform infrared spectroscopy study of the environment of phosphate ions in the early deposits of a solid phase calcium phosphate in bone and enamel and their evolution with age: 2. Investigations in the ν_3 PO_4 domain. Calcif Tissue Int 1991;49:383–388.
33. Walters MA, Leung YC, Blumenthal NC, LeGeros RZ, Konsker KA. A raman and infrared spectroscopy investigation of biological hydroxyapatite. J Inorg Biochem 1990;39:193–200.
34. Boskey AL. Amorphous calcium phosphate: the contention of bone. J Dent Res 1997;76:1433–1436.
35. Paschalis EP, Betts F, DiCarlo E, Mendelsohn R, Boskey AL. FTIR microscopic analysis of normal human cortical and trabecular bone. Calcif Tissue Int 1997;61:480–486.
36. Biltz RM, Pellegrino ED. The nature of bone carbonate. Clin Orthop Rel Res 1977;129:279–292.
37. LeGeros RZ. Apatite crystallines: effect of carbonate on morphology. Science 1967;155:1409–1411.